

# Unveiling Single-Bit-Flip Attacks on DNN Executables

Yanzuo Chen  
*HKUST*

Zhibo Liu<sup>†</sup>  
*HKUST*

Yuanyuan Yuan<sup>†</sup>  
*HKUST*

Sihang Hu  
*Huawei Technologies*

Tianxiang Li  
*Huawei Technologies*

Shuai Wang<sup>‡</sup>  
*HKUST*

## Abstract

Recent research has shown that bit-flip attacks (BFAs) can manipulate deep neural networks (DNNs) via DRAM Rowhammer exploitations. Existing attacks are primarily launched over high-level DNN frameworks like PyTorch and flip bits in model weight files. Nevertheless, DNNs are frequently compiled into low-level executables by deep learning (DL) compilers to fully leverage low-level hardware primitives. The compiled code is usually high-speed and manifests dramatically distinct execution paradigms from high-level DNN frameworks.

In this paper, we launch the first systematic study on the attack surface of BFA specifically for DNN executables compiled by DL compilers. We design an automated search tool to identify vulnerable bits in DNN executables and identify practical attack vectors that exploit the model structure in DNN executables with BFAs (whereas prior works make likely strong assumptions to attack model weights). DNN executables appear more “opaque” than models in high-level DNN frameworks. Nevertheless, we find that DNN executables contain extensive, severe (e.g., single-bit flip), and transferable attack surfaces that are not present in high-level DNN models and can be exploited to deplete full model intelligence and control output labels. Our finding calls for incorporating security mechanisms in future DNN compilation toolchains.

## 1 Introduction

Recent years have witnessed increasing demand for applications of deep learning (DL) in real-world scenarios. This demand has led to extensive deployment of deep neural network (DNN) models in a wide spectrum of computing platforms, ranging from cloud servers to embedded devices. To date, a promising trend is to use DL compilers to compile DNN models in high-level model specifications into optimized machine code for a variety of hardware backends [12, 42, 63].

Hence, instead of being interpreted in frameworks like PyTorch, DNN models can be shipped in a “standalone” binary format and executed directly on CPUs, GPUs, or other hardware accelerators. More and more DNN executables have been deployed on mobile devices [30, 47, 48, 54] and cloud computing scenarios [3, 76].

Despite the prosperous adoption of DNN executables in real-world scenarios, its attack surface is largely unexplored. In particular, existing research has demonstrated that bit-flip attacks (BFAs) enabled by DRAM Rowhammer (RH) are effective in manipulating DNN models [28, 58]. However, existing works only launch BFAs toward DNN models in DL frameworks like PyTorch. Since DNN models executed as low-level machine code have distinct execution paradigms, runtime systems, and more “obscure” code formats than those in the DL frameworks, it is highly timely that a systematic study on the attack surface of BFAs on DNN executables be conducted. To this end, our work provides the first and in-depth understanding of the severity of BFAs on DNN executables, whose findings suggest the need to incorporate comprehensive mechanisms in DNN compilation toolchains to harden real-world DNN executables against exploitations.

We identify practical attack vectors that exploit the model structures in DNN executables (often stored in the `.text` section in DNN executables) with BFAs. Previous attacks rely on rather strong assumptions of the knowledge of full model details. In contrast, we make a practical assumption that the attacker only knows the model structure, which is usually public or recoverable [7, 29, 79]. Thus, benefiting from mechanisms that maximize memory utilization on commercial clouds (e.g., Kernel Same-Page Merging [4]), we unveil that BFAs can be launched in a cross-virtual-machine (cross-VM) manner. We also propose a set of strategies to enable effective and efficient BFAs on DNN executables. We particularly show that, a “vulnerable bit” searcher can be launched over DNN executables sharing the same model structure with the victim DNN executable, which automates the process of locating vulnerable bits in a given DNN executable. Moreover, we adopt and augment an RH attack technique [33] to launch

<sup>†</sup>These authors contributed equally to this work.

<sup>‡</sup>Corresponding author

exploitations on DNN executables deployed on real-world DDR4 devices.

Our extensive study is conducted over DNN executables emitted by two commonly used production DL compilers, TVM [12] and Glow [63], developed by Amazon and Facebook, respectively. We assess the attack surface on diverse combinations of different configurations, including DNN models, datasets, and compilation options, covered by a total of 21 DNN executables in this study. We made important observations, including 1) *Pervasiveness*. We identify on average 16,599 vulnerable bits in each of the DNN executables we studied, even for quantized models, which have been known to be more robust than full-precision models [28, 78]. 2) *Effectiveness & Stealthiness*. 71.1% of the RH attacks reported in this work succeed with only a single bit flip, while 95.6% succeed within 3 flips, making RH attacks highly effective in practice. 3) *Versatility*. We show that BFAs can achieve various attack end-goals over both classification and generative models. 4) *Transferability*. We also find many “super-bits” — vulnerable bits that exist across the `.text` section of DNN executables sharing the same structure but with different weights. We further conduct reverse engineering and manual analysis to characterize those vulnerable bits. Our work highlights the need to incorporate security mechanisms in future DNN compilation toolchains to enhance the reliability of real-world DNN executables against exploitations. In summary, we contribute the following:

- This paper launches the first in-depth study on the attack surface of DNN executables under BFA, one major and practical hardware threat toward DNN models.
- We show how BFAs can be carried out in realistic, cross-VM scenarios. We extend de facto RH techniques on DDR4 devices and design a novel vulnerable bit searcher to automate locating vulnerable bits.
- Our empirical findings uncover the pervasiveness, stealthiness, versatility, and transferability of BFA vectors on DNN executables. We show that DNN executables contain severe attack surfaces that are not present in corresponding DNN models in high-level DL frameworks.

## 2 Preliminary and Related Works

### 2.1 DL Compiler and DNN Executable

**DNN Compilation.** DL compilers typically accept a high-level description of a *well-trained* DNN model, exported from DL frameworks like PyTorch as their input. During the compilation, DL compilers often convert the DNN model into intermediate representations (IRs) for optimizations. High-level, platform-agnostic IRs are often graph-based, specifying the DNN model’s computation flow. Platform specific IRs, such as TVM’s TensorIR and Glow’s High Level Optimizer (HLO), specify how the DNN model is implemented on a specific hardware backend and support hardware-specific op-

timizations. Finally, DL compilers convert their low-level IRs into assembly code (or first into standard LLVM/CUDA IR [37, 46]) for execution.

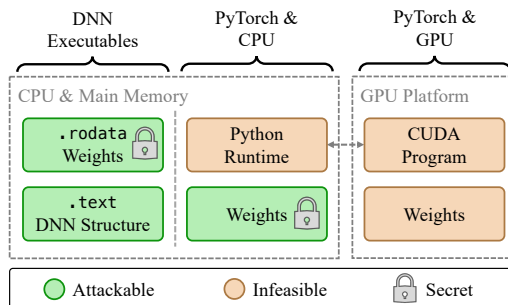


Figure 1: Comparing the runtime systems of DNN models in DL frameworks and DNN executables. Different from prior work, we assume the trained weights are unknown to attackers and thus marked as “secret.”

**DNN Executable and Runtime.** Popular DL compilers like TVM [12] and Glow [63] emit DNN executables in the standard ELF format and can be executed on mainstream CPUs and GPUs. The emitted DNN executables can be in a standalone executable or a shared library (a `.so` file that can be loaded by other programs). Without loss of generality, we focus on the `.so` format in this paper, but our attack pipeline and findings can be easily extended to standalone executables. Fig. 1 compares deploying DNN executables in CPU & main memory with running DNN models in PyTorch. Typically, a DNN executable contains all computation logic of a DNN model in a single executable. DNN executables show a distinct paradigm compared to DL frameworks that essentially interpret the DNN model in a computational graph and offloads low-level computation to external kernel libraries like cuDNN [13] and MKL-DNN [31] on GPUs and CPUs.

As will be reviewed later, existing BFAs on DL frameworks (e.g., [28, 58]) primarily target pre-trained weights of DNN models (which are secret in our assumption, marked using the gray locker in Fig. 1). Moreover, to locate vulnerable bits in model weights, prior works often use gradient-based searching and thus require model weights to be known to the attacker. On the other hand, launching hardware exploitations toward interpretation-based environments is an open problem [52] since the Python runtime contains a more obscure runtime environment, and it is much harder, if not infeasible, to identify BFA vectors in it. Also, it is unclear if GPU memories are vulnerable to BFAs. In contrast, this research analyzes the attack vectors in DNN executables, particularly their `.text` sections (the 2nd “attackable” box) that contain the model structure information. As noted in Sec. 3, we assume that the `.rodata` section, which often contains the model weights, is unknown (“secret”) to the attacker.

**Real-World Usage.** The real-world usage of DL compilers and DNN executables has been illustrated in recent research [12, 32, 42, 63] and industry practice. The TVM com-

munity has reported that TVM has received code contributions from many companies, including Amazon, Facebook, Microsoft, and Qualcomm [15]. TVM has been used to compile DNN models for CPUs [32, 41]. Facebook has deployed Glow-compiled DNN models on CPUs [45]. Overall, DL compilers are increasingly vital to boost DL on CPUs, embedded devices, and other heterogeneous hardware backends [3, 76]. This work exploits the output of DL compilers, i.e., DNN executables, and we, for the first time, show the pervasiveness and severity of BFA vectors in DNN executables.

## 2.2 Bit-Flip Attacks

**BFA via Rowhammer Attack.** BFA is a type of hardware fault injection attack that corrupts the memory content of a target system (by flipping its bits). While BFA can be initialized via a variety of hardware faults [16], RH [35] manifests as one highly effective, practical, and controlled fault injection attack. In short, RH exploits DRAM disturbance errors, such that for some modern mainstream DRAM devices, repeatedly accessing a row of memory can cause bit flips in adjacent rows. RH roots in the fact that frequent accesses on one DRAM row introduce voltage toggling on DRAM word lines. This results in quicker leakage of capacitor charge for DRAM cells in the neighboring rows. If sufficient charge is leaked before the next scheduled refresh, the memory cell will eventually lose its state, and a *bit flip* is induced. As a result, by carefully selecting neighboring rows (aggressor rows) and intentionally performing frequent row activations (“hammering”), attackers can manipulate some bits without directly accessing them.

To date, RH attacks have been successfully applied to a variety of systems, such as kernel memory regions and browsers [14, 21, 33, 35, 65, 72]. It has also led to the rise of corresponding security mitigation techniques [25, 34, 73, 75]. For DDR3 DRAM, RH attacks are most commonly launched by alternating accesses to the two rows adjacent to the victim row (“double-sided hammering”). However, DDR4 DRAM devices have been widely deployed for many years, and due to the implementation of on-chip RH mitigations such as Target Row Refresh (TRR) [19], techniques applicable to DDR3 are no longer effective. More recent research has pointed out that, to launch RH on DDR4, attackers need to precisely control the frequency-domain parameters (phase, frequency, and amplitude) of the hammering procedure in order to induce bit flips [33], which is much more challenging than DDR3. While contemporary BFA research is mostly demonstrated on DDR3 DRAM devices, this work demonstrates RH attacks on recent DDR4 DRAM devices; see Sec. 5.1.

**BFA over DNN.** Recent research has specifically launched BFA toward DNN models [11, 28, 58–61, 78]. The attack goals of BFAs can be generally divided into two categories: first, BFA may be launched to extensively manipulate model predictions over all inputs, possibly reducing the model accuracy to random guesses. In contrast to typical DNN training that

aims to minimize the loss, BFA strives to maximize the loss function  $\mathcal{L}$  to temper inputs [58, 78]. Meanwhile, targeted BFA (T-BFA) aims to manipulate prediction output over specific inputs [60]. T-BFA retains the original predictions over the other inputs to offer a stealth attack. Therefore, existing works primarily launch BFA to flip bits in the model weights. For example, ProFlip [11] identifies and flips the weights of specific salient neurons to extremely large values, which can control the overall predictions for certain classes.

RH attacks are inherently costly, and launching extensive amounts of RH attacks may cause obvious hardware fault and be detected [25, 34, 73, 75]. With this regard, recent BFA-based research strives to manipulate model predictions while flipping as few bits as possible. Prior works have shown gradient-based bit search methods [5, 11] can facilitate both BFAs with varying end goals to identify a small set of bits that, once flipped, can satisfy the attack objectives. The bit search methods often perform intra-layer bit searching toward a layer  $l$ , and then identify the top  $n$  weights the largest gradients as important. Given that weights are stored as floating-point numbers, BFA often flips the bits of the exponent part of those weights to maximize the impact of bit flips.

**BFA over Quantized DNN.** Recent BFA (with different end goals) are increasingly demonstrated on quantized DNN models, mainly because quantized DNN models are, by design, more robust and harder to attack by BFA [57, 78]. More specifically, quantized DNN models are created by mapping the original floating-point weights and computations to their discrete, integer versions. This way, the possible ranges for numerical values inside quantized models are significantly compressed (usually down to 8-bit integers), and bit flips occurring in model weights have a much more limited impact on the overall model behavior. Recent research has also shown that it takes more bit flips to achieve the same attack objectives on quantized DNN models than on their floating-point versions (2x to 23x more bit flips) [78]. In this work, we show that quantization does not grant DNN executables more robustness against BFAs, and we can still successfully deplete their intelligence by flipping a single bit, as shown in Sec. 7.5.

## 3 Threat Model and Assumptions

**Environment.** Our attack targets DNN executables compiled by DL compilers. We assume that the attackers are able to perform BFA using currently mature RH exploitation techniques on the DRAM of a host. Moreover, we for the first time illustrate the feasibility of launching practical cross-VM BFAs on DNN executables; see relevant assumptions and details in Sec. 5.1. For the attacker, the steps for RH include memory templating [62], memory massaging [65, 71], and hammering. Our assumption is reasonable and shared by prior BFAs over DNN models. Often, the attacker can place a malicious program on a PC or cloud host machine co-located with the victim DNN executable, then launch RH [28, 75, 78]

attacks while not requiring any software-level vulnerabilities on the victim DNN executables or the attack host. Moreover, launching hardware attacks does not involve preparing malicious DNN inputs (“adversarial examples” [20]) and feeding them to the victim DNN executables. The victim DNN executable exposes its public interface (e.g., for medical image diagnosis); while the attacker does not need to interact with the victim DNN executable, she can query its outputs via its public interface during RH.

**Knowledge of the Victim DNN Model.** Our attack is distinct from *all* prior BFAs in terms of knowledge of the victim DNN model. Existing works generally assume that attackers have full knowledge of the victim DNN model, including the model structure and the trained weights [5, 11, 56, 59, 75, 78]. For example, DeepHammer [78] requires the trained weights to compute gradients. Nevertheless, we deem this is an overly strong assumption: DNN weights are generally trained on private data and viewed as the key intellectual property of DNNs. In practice, only DNN owners have access to the trained weights, and no existing (query-based model extraction) attacks can fully recover DNN weights.<sup>1</sup>

As introduced in Sec. 2, DL compilers generally accept well-trained DNN models and compile them into DNN executables. We assume the only victim DNN model’s structure is known to the attacker. This is more practical because model structures are often fully or partially public.<sup>2</sup> On the other hand, even if the structure is private, recent works have demonstrated the feasibility of successfully recovering the full structures of DNNs [29, 77, 82]; attackers can infer the structure with these techniques before launching BFA. Besides, given that DL compilers only provide very limited compilation settings (e.g., full optimizations and AVX2) compared with traditional C/C++ compilers, we assume that replicating the same compilation setting is not difficult (e.g., by iterating all possible settings to “match” the victim executable). In other words, knowing the model structure and compilation setting, attackers can get the `.text` section of the victim DNN executable, but not the `.rodata` section, as shown in Fig. 1.

Overall, our requirements are quite permissive for the attacker; it is indeed a looser set of assumptions when compared to prior techniques launching BFAs toward DNN models in high-level DL frameworks, which work in a purely white-box scenario. See our attack details in Sec. 5.1.

**Attacker’s Goal.** For DNN models in DL frameworks, their weights are often stored in a so-called “weights file.” Existing works assume the full knowledge of the victim DNN models, and accordingly, they strive to flip bits in that weights file. As noted in Fig. 1, attacking other components appears technically challenging and unscalable [52]: DNN models are

<sup>1</sup>Query-based model extraction [49, 70] only trains a new DNN of similar *functionality* with the victim DNN on a limited set of inputs; they cannot recover the exact values of DNN weights.

<sup>2</sup>Most commercial DNNs are built on public well-defined backbones, e.g., Transformer [74] is the building block of the GPT models [8].

interpreted in the DL framework, forming a complex runtime environment. Attacking certain bits in the process memory space may likely lead to unexpected behaviors instead of a deterministic attack controlled by the attacker.

In contrast, we show that launching effective and controllable BFAs is feasible against the model structure, i.e., the `.text` section of the victim DNN executable. In fact, this paper uncovers a much larger attack surface than that of a “weights file.” We are the first to consider attacking both classification and generative models. Accordingly, we demonstrate two representative end goals: for classifiers, we successfully downgrade the inference accuracy of the victim DNN model to that of a random guess, and for generative models, we temper the generation results to get biased or messed outputs. As clarified in Sec. 5.1 and empirically shown in Sec. 7.3, our launched downgrading attack can be easily extended to more targeted attacks (often referred to as T-BFA), e.g., manipulating the classification outputs of specific inputs to a target class. In addition, tempered generation results can consequently result in model poisoning attacks when used in data augmentation [9, 43, 66]. While adversarial example inputs [20] are deliberately crafted to mislead DNN models, our attacks make DNN models mal-functional when provided with normal, legitimate inputs.

## 4 Attack and Key Findings Overview

We first present the attack overview. As mentioned earlier, we require that the attacker has a DNN executable that shares identical DNN structure with the victim DNN executable. This enables the attacker to conduct offline bit searching and identify that are highly likely vulnerable (details in Sec. 5). Our bit searching is an offline process, meaning that the attacker can perform it in a local simulation environment, where the attacker can easily perform BFAs at will (see details in Sec. 5.1). In contrast, once bit searching is finished, the online attack is conducted via RH exploitation in the real-world environment; we successfully demonstrate the feasibility of the attack on a mainstream DDR4 DRAM by following and extending a state-of-the-art RH exploitation technique [33]. Before presenting the attack details, we first introduce the key findings of this research, whose corresponding empirical studies are presented in Sec. 7.

① **Pervasive Vulnerabilities in DNN Executables.** DNN executables compiled by mainstream DL compilers, TVM and Glow, are pervasively vulnerable under BFAs. Moreover, with reverse engineering and extensive manual efforts, we present characteristics of the vulnerable bits in Sec. 7.6, illustrating that vulnerable bits can originate from various binary code patterns that commonly exist in DNN executables.

“Reflections on Trusting Trust”: *Compiler-Introduced Backdoors.* Following ①, comparing with DNN models in high-level DL frameworks, we confirm that the vulnerable bits we found in DNN executables do not exist in their correspond-

ing DNN models in high-level DL frameworks. We view these shared, common issues as hardware “backdoors” introduced by DL compilers and the runtime, which conceptually correlates to the classic backdoor attack noted in Ken Thompson’s Turning award lecture [69] — “Reflections on Trusting Trust.” This observation advocates for low-level, binary-centric security analysis and mitigation against BFAs, for which today’s BFA mitigation techniques that mainly focus on model weights and are deployed in DL frameworks [75, 81], are hardly applicable.

② **Transferable “Superbits.”** By assuming a relatively weak attacker (knowing model structure but not weights), our attack pipeline benefits from “transferability,” where attackers locally profile a set of DNN executables that share identical `.text` section with the victim and apply the identified vulnerable bits in the local DNN executables to the remote victim DNN executable. We find that those identified vulnerable bits are often applicable to the victim DNN executable which shares the same structure. This illustrates an important finding that many subtle yet common attack surfaces exist in DNN executables. For simplicity, we name those common vulnerable bits “superbits,” indicating that those bits are applicable to multiple DNN executables sharing the same model structure, allowing adversaries to launch rapid, transferable attacks under realistic settings.

③ **Effective & Stealthy Corruption.** Moreover, we show important findings that DNN executables can be easily corrupted by BFAs via flipping *a single bit*. In contrast, when attacking DNN models in DL frameworks, prior works often need to mutate a dozen of bits to achieve reasonably high attack success rates. Note that mutating a single bit shall largely enhance the *stealthiness* of our attack, meanwhile reducing the cost and making the attack more practical when conducting RH on real-world devices. To date, launching BFA via RH attacks is very costly, and by only mutating a single bit, we successfully demonstrate effective attacks on a mainstream DDR4 device. See Sec. 7.2 and Sec. 7.5 for results.

④ **Versatile Exploitation.** We also show that DNN executables can be exploited with various end goals. In addition to contemporary works that downgrade DNN classifier accuracy via BFA, we also demonstrate attacking generative models via BFA (see evaluations in Sec. 7.3). This reveals a new attack angle and severe consequence of our attack: generative models are often adopted for data augmentation (e.g., for medical image analysis [9, 18, 22, 43, 68]), and manipulating the generated images can introduce bias into the augmented datasets and consequently make the augmented DNN biased. For example, by leveraging BFA, we can make a chest X-ray image generator always generate benign X-ray images. As a result, the DNN augmented using this manipulated dataset will tend to predict most inputs as “benign.”

⑤ **Practical Exploitation.** An important distinction between our exploitation and previous works is that we directly exploit the `.text` section in the DNN executables, whereas

prior works target the victim DNN’s weights file stored on DRAM [78]. Similarly, recent defense mechanisms mainly focus on protecting the weights files [75, 81], which are not directly applicable to our attack. We have clarified the validity of this assumption in Sec. 3. Our attack, over all studied victim executables, is successfully demonstrated on mainstream DDR4 DRAMs whereas previous DNN-oriented BFAs only show their attack on DDR3 DRAMs.

## 5 Design

We present our attack pipeline in Sec. 5.1. Sec. 5.2 discusses the rationale and tactic of obtaining “well-trained” DNN executables, which is employed in offline bit searching (Sec. 5.1).

### 5.1 BFA Pipeline

**Conditions for Vulnerable Bits.** Let the victim DNN model be  $f_\theta$ , where  $\theta$  denotes its weights and  $f$  denotes its structure. We also use  $e$  to represent the executable of  $f_\theta$  compiled by a DL compiler. Before starting the attack, the attacker first decides what kind of bits are considered “vulnerable.” For simplicity, we assume the following conditions: If the attacked DNN is a classifier, vulnerable bits are those that cause the inference accuracy of the classifier to drop to a random guess ( $\approx \frac{1}{\#\text{classes}}$ ). If the attacked DNN is a generative model, vulnerable bits cause its output image quality or semantics to drastically change (see details in Sec. 7.1). In either case, vulnerable bits *cannot* cause the DNN to crash. Moreover, since this paper focuses on *single-bit* BFAs in DNN executables (as opposed to prior works that chain multiple bit flips to achieve the same effect [57, 78]), we add that, any vulnerable bit *must* meet the above conditions solely on its own. We also follow these settings in our evaluation later in Sec. 7. Fig. 2 depicts our attack pipeline which consists of three steps:

**Offline: Bit Searching.** As mentioned in Sec. 3, we assume that the attacker has no knowledge about the weights  $\theta$  or training data of the victim model  $f_\theta$ ; she must rely on what she knows, namely the model structure  $f$  and the compilation setting, to determine which bits inside the victim executable  $e$ ’s `.text` region to attempt to flip. We achieve this with a novel offline bit search method. In short, the attacker first locally prepares a series of  $n$  DNN executables  $\mathcal{E} = \{e_1, e_2, \dots, e_n\}$ , where each  $e_i \in \mathcal{E}$  shares the identical structure with the victim DNN  $e$  but with different weights.

We require that weights in each  $e_i$  are well trained (noted as “trained weights;” see Sec. 5.2 for details). In other words, the weights must be the output of a training process with an optimizer, instead of being randomly initialized. This is because DNNs with trained and randomly initialized weights have different behavior patterns, and flipping the same bit in `.text` typically causes distinct consequences for their predictions. Obtaining enough trained weights is inherently challenging, as attackers usually have a limited number of real-

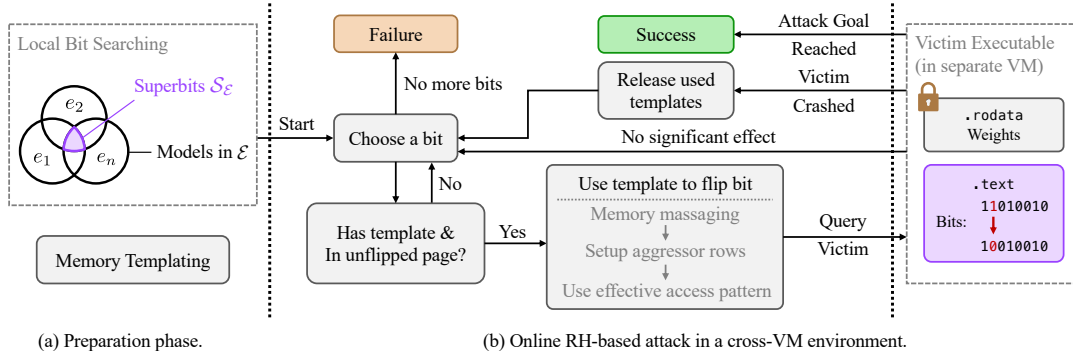


Figure 2: The attack pipeline. The “lock” symbol in the top right means attackers cannot access the weights of the victim.

world datasets with distinct features. Thus, we obtain trained weights in a novel data-free manner; see details in Sec. 5.2.

After obtaining  $\mathcal{E}$ , the attacker starts to use them as local profiling targets. Ultimately, our goal is to find vulnerable bits in  $e$  that can be flipped to cause a desired effect, but this is challenging because it is normally hard to tell whether an arbitrary bit will be a vulnerable bit in the victim executable  $e$  whose weights are never exposed to the attacker. Recall that, as introduced in ② of Sec. 4, we identify superbits that are transferable among DNN executables with distinct weights; attacks can leverage this transferability to search for vulnerable bits. More specifically, searching for vulnerable bits in the victim  $e$  can be transformed to finding superbits shared by  $\mathcal{E}$  that are likely also shared by  $e$ ; we give details below.

For each  $e_i \in \mathcal{E}$ , if the attacker obtain a set of its vulnerable bits  $\mathcal{V}_i$ , she can then calculate the superbits over  $\mathcal{E}$ , denoted as  $\mathcal{S}_{\mathcal{E}} \stackrel{\text{def}}{=} \bigcap_{i=1}^n \mathcal{V}_i$ , illustrated in Fig. 2(a). As the size of  $\mathcal{E}$  increases,  $\mathcal{S}_{\mathcal{E}}$  becomes a set of superbits that are shared by more and more  $e_i$ ’s. Intuitively, these superbits are also more likely to affect the victim  $e$  as well, since  $e$  has the same model structure as  $e_i$ . Although the superbits’ vulnerability in  $e$  is not guaranteed and the attacker will not know until she launches the online attack towards  $e$ , our empirical results show that this approach finds vulnerable bits in  $e$  with high enough accuracy for real-world attackers to conveniently launch practical attacks, as we will demonstrate in Sec. 7.5.

To obtain  $\mathcal{V}_i$  for every  $e_i$ , a naïve attacker would need to sweep all bits in each  $e_i$ ’s `.text` section and check if the vulnerability condition is met, then repeat this process for all  $e_i \in \mathcal{E}$ . However, this can be very time-consuming, especially for complex DNNs that can have more than 6.8 million bits in their `.text` sections, according to our preliminary study. To speed up the search, the sweeping process and intersection calculation can be interleaved so that the attacker can iteratively shrink  $\mathcal{S}_{\mathcal{E}}$ , starting with  $\mathcal{S}_{\mathcal{E}} = \mathcal{V}_1$ , each iteration trying the bits already in  $\mathcal{S}_{\mathcal{E}}$  on an unswept binary  $e'$  and removing those that are not vulnerable in  $e'$ , instead of trying all bits in  $e'$ . During this process, the attacker will need to flip bits in the local executables  $\mathcal{E}$  and assess their effects. We clarify

that this is simple: as the attacker has full control over  $\mathcal{E}$  and her local environment, she can easily achieve bit flipping by editing the binary files.

**Online Preparation: Memory Templating.** Our attack is achievable in practical and challenging settings: we consider the attacker and victim to be in separate VMs on the same multi-tenant cloud server so they cannot access each other’s files or processes, as in typical machine-learning-as-a-service (MLaaS) environments. As a “warm up,” the attacker needs to scan the DRAM module in the host machine for bit locations that can be flipped using RH, a procedure called memory templating [62]. A bit is flippable using RH only if there is a “template” in the DRAM module with the same bit location and flip direction. Moreover, for DDR4 platforms, an effective “DRAM access pattern [33]” containing the frequency-domain information needed to launch RH on the platform must also be found and applied to trigger a flip. The set of metadata describing where RH can flip bits and how to flip each bit are called *memory templates*. Currently, multiple tools have been made available to find these templates on DDR4, including Blacksmith [33] and TRRespass [19]. In our pipeline, we leverage and slightly extend Blacksmith, the state-of-the-art RH technique for DDR4, to perform memory templating and use the access patterns it found in the attack step later.

**Online Attack: RH.** Since the attacker and victim are in two different VMs on the same host, we also assume that Transparent Huge Page (THP) and memory deduplication is enabled on the host, as done commonly to maximize the memory utilization in a commercial environment [2, 23, 64]. Here, memory deduplication refers to techniques such as Kernel Same-Page Merging (KSM) on Linux or Transparent Page Sharing (TPS) on VMware ESXi, both of which identify and merge identical memory pages across different virtual machines. During the attack, KSM and TPS would merge the pages containing the `.text` section of  $e$  and any binary in  $\mathcal{E}$  because these pages are *identical*. This enables a unique opportunity for the attacker to modify bits in  $e$  because, by flipping the bits in a merged page, the modification will also be directly visible in the victim’s page, bypassing any software protections such

as copy-on-write (CoW) that is normally triggered when the content of a merged page is modified through OS APIs.

Nevertheless, if the host has disabled THP or memory deduplication (rare in practice), the attacker can still exploit the vulnerable bits in  $e$  in line with previous work’s threat model that assumes co-location of the attacker and victim [78].

After the attacker has determined the set of superbits  $\mathcal{S}_E$ , she can launch RH to flip the vulnerable bits in  $e$ . She does so by first choosing a superbit  $s \in \mathcal{S}_E$  that has at least one available template, whose information has been obtained in the “warm-up” phase. Then, as shown in Fig. 2(b), she also needs to check if the bit belongs to an unflipped page: Due to the implementation of KSM, the attacker can only flip one bit per merged page [62], unless the victim executable crashed and restarted, in which case its associated memory is considered to be reset. If all these requirements are met, the attacker can then use the template to flip the bit via standard RH, whose steps include memory massaging, setting up aggressor rows, and applying the effective access pattern. Here, memory massaging refers to the process of precisely placing the memory page containing the bit to flip at the location specified by the template, and can be done via one of the many existing techniques [36, 62, 65, 71, 78] according to the attacker’s need.

Overall, after the bit flip is triggered by RH, the attacker queries the victim executable via its public interface to check if its behavior has changed as expected. As shown in Fig. 2(b), there are three possible outcomes: (1) the victim’s behavior changes as expected, which is the desired outcome; (2) the victim crashes, which is undesirable since attackers wish to manipulate the victim’s behavior without crashing it; and (3) the victim’s behavior does not change, which is also undesirable. In the latter two cases, the attacker has to repeat the above process with a different superbit  $s$  until she finds a bit that can be flipped and changes the victim’s behavior as expected, or runs out of possible superbits to try.

Our attack can be directly performed on DDR4 DRAM, and does not require any hardware modification. Moreover, we clarify that this step is not limited to Blacksmith, and can be replaced by any other RH techniques if needed [21, 35, 40].

## 5.2 Preparing Well-Trained Weights without Distinct Training Datasets

Following the discussion of the need for trained weights in Sec. 5.1, this section elaborates on their definition, the reason and challenges for getting them, as well as how we efficiently and effectively obtain a set of  $\mathcal{E}$  where each  $e_i \in \mathcal{E}$  has well-trained weights, even when  $|\mathcal{E}|$  is large (e.g., about ten).

**DNN Functionality.** We start by formulating a DNN’s functionality. In general, a DNN  $f_\theta : \mathcal{X} \rightarrow \mathcal{Y}$  can be viewed as a parameterized function mapping an input  $x \in \mathcal{X}$  to an output  $y \in \mathcal{Y}$ . For example, mapping an image to a label for image classifiers. The DNN structure (denoted by  $f$ ) is a non-linear

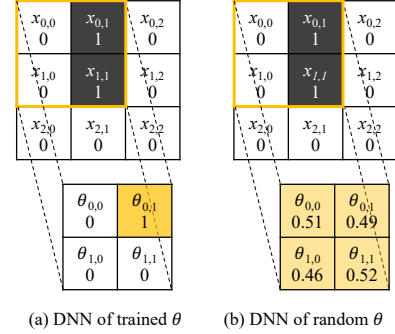


Figure 3: Comparing DNNs with trained/random weights  $\theta$ .

function, whereas the weights  $\theta$  are learned from training data, implicitly representing the rules for mapping  $\mathcal{X}$  to  $\mathcal{Y}$ .

---

### Algorithm 1: Execution of a Sample Conv DNN.

---

```

1 function Conv2D_DNN(x, theta):
2   kernel ← [2, 2]; stride ← 1;
3   out ← 0;
4   for i ← 0 to 3 - kernel[0] by stride do
5     for j ← 0 to 3 - kernel[1] by stride do
6       for k ← 0 to kernel[0] - 1 by 1 do
7         for l ← 0 to kernel[1] - 1 by 1 do
8           out ← out + xi+k, j+l * thetak, l;
9         end
10      end
11    end
12  end
13  out ← ReLU(out);
14  return out > 0;

```

---

**Well-Trained vs. Randomly-Initialized Weights.** A group of well-trained weights  $\theta$  should encode a fixed mapping (implicitly) defined by the training data. Also, because the randomness (i.e., entropy) in weights gradually reduces during training [6, 17, 39, 50], the trained mapping typically focuses more on some input elements while caring less about others (i.e., have preferences). This distinguishes a well-trained DNN from a DNN with randomly initialized weights: the latter usually treats different input elements approximate equally.<sup>3</sup> We give the definition of trained weights below.

We illustrate this in Fig. 3, where we show the computation of the same convolutional DNN (see line 4–12 in Alg. 1) with trained weights (Fig. 3(a)) and randomly initialized weights (Fig. 3(b)). When given the same input  $x$ , the trained weights focus only on  $x_{0,1}$ ,  $x_{0,2}$ ,  $x_{1,1}$ , and  $x_{1,2}$  because only  $\theta_{0,1}$  is non-zero, whereas the randomly initialized weights treat all input elements  $x_{0,0}$ – $x_{2,2}$  approximately equally.

We now make the connection to show why this difference is important for BFAs on DNN executables: although Fig. 3 shows the same DNN model  $f$  just with different weights, when compiled into DNN executables, they will have distinctly distributed vulnerable bits. Consider the execution process of the Fig. 3 (see Alg. 1). For the trained weights (Fig. 3(a)), skipping either of the two inner loops (line 6 and

<sup>3</sup>That’s why it performs random predication. Note that this “equal” case is associated with the highest entropy (randomness).

7)<sup>4</sup> will change the value of *out* to 0. As a result, the prediction output changes from *true* to *false*. In contrast, if randomly initialized weights (Fig. 3(b)) are used, the prediction function will still have the same output after the same mutation.

On the other hand, for different trained weights that have distinct preferences (e.g., those having larger weight values on  $\theta_{0,0}$ ,  $\theta_{1,0}$ , or  $\theta_{1,1}$ ), all of them have vulnerable bits on line 6 and 7 in Alg. 1. These transferable bits (i.e., superbites) among different DNN executables can be leveraged to conduct real attacks. More concretely, if we have identified some vulnerable bits on line 6 and 7 which are shared by multiple executables of different trained weights, we have high confidence that these bits are also vulnerable in the victim executable (and we empirically show this in Sec. 7.5). Therefore, we argue that superbites  $\mathcal{S}_{\mathcal{E}}$  found over a set of executables  $\mathcal{E}$  with trained weights are more likely to be also shared by the victim executable which we reasonably assume to also have trained weights (since they are adopted for real applications).

As a result, we require that offline profiling must use a set of DNN executables  $\mathcal{E}$  where each of them has well-trained weights rather than randomly initialized weights.

**Constructing Fake Datasets.** Given usually the limited number of datasets, the key challenge at this step is preparing trained weights encoding distinct mappings/preferences. Note that training weights of different values on the same dataset (e.g., by varying training setups) is infeasible because their encoded mappings will be similar (since mappings/preferences are learned from the same training data). As a result, the searched vulnerable bits will be biased and unable to transfer among weights trained on unknown datasets.

One unique opportunity, as observed in our study, is that the mapping encoded in a DNN is not necessarily semantically meaningful (e.g., perform a reasonable classification). Since we only focus on the distinction between mappings, it is unnecessary to train weights on different *real datasets*. Previous works in the machine learning community have shown that, pre-training DNNs with random datasets can speed up the follow-up fine-tuning on real meaningful datasets, because during the pre-training, DNN weights are “regulated” to be similar to those trained on real datasets [44, 51]. Inspired by this observation, we use random noise to construct fake datasets of distinct mappings. To do so, we first randomly generate random noise as inputs and assign labels for them. Once this step is done, the inputs and their labels are fixed; a fake dataset is therefore constructed. Then, when training with a fake dataset, a randomly initialized weight is gradually updated to encoding the mapping in the fake dataset, and certain preferences are accordingly formed. Since the mappings in different fake datasets are completely different, DNN weights of distinct preferences can be obtained by training using different fake datasets.

<sup>4</sup>For simplicity, we omit the discussion on whether this is possible via BFA here; we show various ways BFA can corrupt machine code in Sec. 7.6.

## 6 Study Setup

**DL Compilers.** This research uses two DL compilers, TVM (version 0.9.0) and Glow (revision b91adff10), which are developed by Amazon and Meta (Facebook), respectively. To the best of our knowledge, these two DL compilers represent the best DL compilers with broad application scope and support for various hardware platforms. Both DL compilers are studied in the standard setting without any modifications. TVM allows users to specify the optimization level, and we study both the lowest optimization level (-00) and the highest optimization level (-03). Moreover, we also study the effect of the AVX2 switch, which controls whether the generated code uses AVX2 instructions, on the attack surface of BFAs. This is because these instructions allow many vectorized calculation optimizations and are widely used in DNNs to accelerate computation; we confirm that TVM emits binaries with different ASM instructions with and without this switch. On the other hand, Glow does not allow users to specify the optimization level, and it enables full optimizations by default. Sec. 2.1 has clarified the high-level workflow of DL compilation. TVM and Glow compile DNN models into standalone 64-bit x86 executables that can be directly executed on CPUs.

**DNN Models and Datasets.** This research uses five representative DNN models. We pick ResNet50, GoogLeNet, DenseNet121, and LeNet, four popular image classification models, all of which are widely-used with varying model structures and a diverse set of DNN operators. Each of them has up to 121 layers with up to 23.5M weights. In addition, we also include the quantized versions of these models to evaluate whether their robustness against traditional weights-based BFAs still holds as DNN executables. However, we do not compile quantized models with Glow, because Glow has no support for them. To explore BFAs on generative models, we focus on generative adversarial networks (GANs) as they are the most popular ones. We select DCGAN, which is the backbone of nearly all modern GANs.

For the image classification models, we train them on three popular and representative datasets, CIFAR10, MNIST, and Fashion-MNIST. For DCGAN, we train it on the MNIST dataset and evaluate its outputs in aspects of image quality and semantics. These trained models, after being compiled as executables, are treated as the victim for attacks. With different compilers and configurations, we have 21 victim DNN executables as listed in Table 2. As noted in Sec. 5.2, for our practical attack experiments (see Sec. 7.5), we require DNNs trained on fake datasets for local profiling. To do so, we train each DNN on ten fake datasets for offline bit searching.

Table 1 lists all seed DNN models, their numbers of weights and accuracies, as well as the sizes of their compiled executables and the .text sections. We report that the (victim) classification models have average accuracies of 91.34%, 89.68%, 87.53%, and 98.50%, respectively, for all datasets. In terms of file size, executables compiled by Glow are much smaller

than those compiled by TVM, since Glow does not embed the weights data into the executable but instead stores them in a separate file. When weights are embedded into the executables, the file size is generally proportional to the number of weights of the model; this also means that for the quantized variants, the file size is usually much smaller.

As for the size of the `.text` section, it is influenced by both the complexity of the model structure and the enabled compiler options: more complex structures like quantized models and models with more layers tend to have larger `.text` sections, while enabling optimizations reduces the size of the `.text` section. For example, the binary with the largest `.text` section is the quantized DenseNet121 (844.5K), and ResNet50’s `.text` section size reduces from 215.7K to 86.4K after optimizations are enabled.

Table 1: Statistics of DNN models and their compiled executables evaluated in our study.

Model	#Weights	Avg %Acc.	Compiled binaries	
			File size	<code>.text</code> size
ResNet50 [24]	23.5M	91.34	0.3-90.7M	80.8-215.7K
GoogLeNet [67]	5.5M	89.68	6.0-21.4M	221.5-337.9K
DenseNet121 [53]	7.0M	87.53	8.9-27.3M	427.3-844.5K
LeNet [38]	3.2K	98.50	78.0-90.0K	17.7-25.0K
DCGAN [55]	3.6M	-	13.7M	42.4K

## 7 Evaluation

In this section, we report the evaluation results in accordance with the five key findings listed in Sec. 4.

### 7.1 ① Pervasive Vulnerabilities

DNN executables compiled by mainstream DL compilers are extensively vulnerable under BFAs. Table 2 shows the list of binaries we have trained, compiled, and evaluated based on our study setup in Sec. 6. To give an in-depth analysis, we form different comparison groups as follows:

(1) **Model Objectives and Structures.** Overall, for both classifiers and generative models, all models have from about 0.52% to 7.54% (weighted average 2.21%) of their `.text` region bits vulnerable to BFAs where flips each single bit can successfully manipulate model output. Here, we consider a bit vulnerable if flipping it causes an image classification model to degrade to a random guesser (i.e., the accuracy drops to  $\frac{1}{\text{\#classes}}$ ). For a GAN model, if, after flipping a bit, 85% of its outputs’ labels changed or either the Fréchet Inception Distance (FID) [26] or average Learned Perceptual Image Patch Similarity (LPIPS) [80] score becomes higher than their 85th percentile values, we consider the bit vulnerable.

For quantized models, we notice that their percentages of vulnerable bits are significantly lower than their full-precision versions, especially for Quantized GoogLeNet and Quantized DenseNet121, which only have 0.84% and 0.52% of `.text`

Table 2: Vulnerable bits in our evaluated DNN executables.  $\mathbb{Q}$  denotes quantized models. The last two rows are Glow-compiled executables whereas the rest are TVM-compiled. Glow does not have explicit compiler options to config.

Model	Dataset	Compiler Config	#Bits	#Vuln.	%Vuln.	%“0→1”
ResNet50	CIFAR10	O3, AVX2	311808	8091	2.59	63.92
ResNet50	CIFAR10	O0, AVX2	809744	27328	3.37	58.78
ResNet50	CIFAR10	O3	268992	10999	4.09	64.27
ResNet50	MNIST	O3, AVX2	311808	9803	3.14	61.96
ResNet50	MNIST	O0, AVX2	809744	26942	3.33	55.94
ResNet50	MNIST	O3	268992	11832	4.40	64.24
ResNet50	Fashion	O3, AVX2	311808	9585	3.07	58.74
GoogLeNet	CIFAR10	O3, AVX2	903408	23136	2.56	66.49
GoogLeNet	MNIST	O3, AVX2	903408	22665	2.51	64.94
GoogLeNet	Fashion	O3, AVX2	903408	23375	2.59	62.01
DenseNet121	CIFAR10	O3, AVX2	1317424	35109	2.66	62.51
DenseNet121	MNIST	O3, AVX2	1317424	27705	2.10	70.03
DenseNet121	Fashion	O3, AVX2	1317424	30205	2.29	68.32
$\mathbb{Q}$ ResNet50	CIFAR10	O3, AVX2	728712	15846	2.17	55.05
$\mathbb{Q}$ GoogLeNet	CIFAR10	O3, AVX2	1384904	11588	0.84	54.75
$\mathbb{Q}$ DenseNet121	CIFAR10	O3, AVX2	2666280	13944	0.52	57.73
LeNet	MNIST	O3, AVX2	68800	1733	2.52	60.70
LeNet	MNIST	O0, AVX2	102888	2152	2.09	58.36
DCGAN	MNIST	O3, AVX2	220560	16634	7.54	64.64
ResNet50	CIFAR10	NA	414600	10296	2.48	66.24
ResNet50	MNIST	NA	414600	9614	2.32	66.35

- 1) #Bits denotes the total number of bits in the `.text` section.
- 2) #Vuln. is the number of vulnerable bits identified, %Vuln denotes the percentage of vulnerable bits in the total bits, i.e., #Vuln/#Bits.
- 3) %“0→1” indicates the percentage of flipping from bit 0 to 1.

region bits vulnerable, respectively. In a way, this result confirms the observation from prior works that the BFA surface on quantized models is smaller than on full-precision models. However, we also note that because quantized models are significantly more complicated in terms of structure, they produce binaries with much larger `.text` regions after compilation (e.g., for the first ResNet50 binary in Table 2, its quantized version has a `.text` section that is 98,044 bytes larger). Thus, the absolute number of vulnerable bits is still significant (over 10,000), leaving attackers plenty of room to launch attacks.

(2) **Compiler Configurations.** In Table 2, we have two compilers, TVM and Glow, where for the TVM, we also have two options (optimization levels and AVX2 code generation toggle) set to different values. We find that turning off either optimizations or AVX2 will increase the vulnerability of the DNN executable. Since the TVM optimization pipeline simplifies and fuses many operators in the computational graph [12], the large amount of unfused individual operators in an unoptimized executable may introduce more structures vulnerable to BFAs, such as more loops and more exploitable loop variables, hence more vulnerable bits. On the other hand, turning off AVX2 replaces all AVX2 instructions in an executable with simpler SSE instructions, for example replacing `VMOVAPS` with `MOVAPS`. While there have to be more instructions because SSE is less vectorized than AVX2, these new instructions are shorter in machine code, so the binaries’ `.text` regions still shrink, as shown in Table 2. We also noticed that the opcode bits in these SSE instructions are more “flippable” than those in AVX2 instructions, i.e., an opcode is more eas-

Table 3: Top 10 most common flip types in AVX2 and non-AVX2 binaries. “Pct.” stands for percentage.

Rank	AVX2 Binaries		Non-AVX2 Binaries	
	Instruction (Flip Type)	Pct. (%)	Instruction (Flip Type)	Pct. (%)
1	VMOVUPS (Data)	12.34	MULPS (Opcode)	16.96
2	MOV (Data)	8.82	MULPS (Data)	15.96
3	ADD (Data)	6.23	ADDPS (Opcode)	9.12
4	VBROADCASTSS (Data)	5.83	MOV (Data)	8.02
5	VXORPS (Data)	5.17	MOVAPS (Opcode)	5.63
6	VMADD231PS (Data)	4.88	XORPS (Data)	4.88
7	LEA (Data)	4.86	ADD (Data)	4.37
8	VMOVAPS (Data)	3.47	ADDPS (Data)	4.07
9	VADDPS (Opcode)	3.35	MOVAPS (Data)	3.96
10	VADDPS (Data)	3.31	MOVSS (Opcode)	3.78

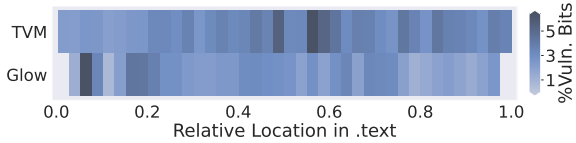


Figure 4: Distribution of vulnerable bits in DNN executables.

ily flipped to become another still *valid* opcode that does something, as can be seen by comparing the most common flip types before and after turning off AVX2 in Table 3. This is likely because shorter instructions have a smaller opcode space, so different opcodes are closer to each other (in terms of Hamming distance).

Additionally, we report that the vulnerable bits are distributed throughout the entire `.text` region of a binary rather than being concentrated in a small region. The distribution of vulnerable bits in the `.text` region is plotted in Fig. 4, where the darkness of the color indicates the portion of vulnerable bits found in the corresponding address range inside `.text`. For Glow, the regions near the beginning and end of the `.text` region are mainly auxiliary functions (e.g., PNG image loading), so we do not consider vulnerable bits in these regions. Other than that, for both TVM and Glow, vulnerable bits are distributed relatively evenly inside `.text`; this translates to higher success rates for attackers, as the “one bit per page” constraint in Sec. 5.1 will have much less impact on them.

## 7.2 ② Effective & Stealthy Corruption

As mentioned in the “conditions for vulnerable bits” in Sec. 5.1, all of our findings are vulnerable bits that can be used to deplete full DNN model intelligence with only a single-bit BFA. For example, flipping bit 1 of the byte at offset `0x1022f6` in the first binary in Table 2 causes the model’s prediction accuracy to drop from 87.20% to 11.00%, equivalent to a random guesser. To the best of our knowledge, this is the first work to report such single-bit corruptions in DNN models. We believe the ability to corrupt a model using one single-bit flip is an important motivation for real-world attackers because, under the assumption that BFAs are mostly instantiated using RH, which is a probabilistic process, it greatly reduces the cost for the attack and increases the success rate, as we will see in our practical attack experiments

in Sec. 5.1. It also largely reduces the risk of being detected by the victim (i.e., more stealthy), as the corruption is much more subtle than the case of multi-bit corruption.

One intriguing fact related to launching single-bit BFA is that the flip direction of the vulnerable bits leans towards  $0 \rightarrow 1$ . Intuitively, a more uniform distribution might be preferred by attackers, so she can maximize her attack opportunities using the observation that vulnerable DRAM modules tend to have about the same amount of  $0 \rightarrow 1$  and  $1 \rightarrow 0$  flips [33, 35]. Given that said, we believe the skewness we found is still in an acceptable range and does not impede attacks, as we will show later.

Table 4: Number of vulnerable bits by output class. The last two rows are Glow-compiled executables whereas the rest are TVM-compiled.

Model	Dataset	#Vulnerable Bits by Output Class									
		0	1	2	3	4	5	6	7	8	9
ResNet50	CIFAR10	742	447	3192	881	121	1509	381	67	249	502
ResNet50	MNIST	12	7699	33	17	8	77	14	150	284	1509
ResNet50	Fashion	0	8543	96	6	2	87	71	19	336	425
GoogLeNet	CIFAR10	1747	2022	8430	1538	614	1814	1088	918	1290	3675
GoogLeNet	MNIST	188	1600	1226	1730	256	2991	2133	526	2062	9953
GoogLeNet	Fashion	6165	388	722	302	2989	1123	505	1366	417	9398
DenseNet121	CIFAR10	604	23425	1681	1881	2328	504	1321	234	1913	1218
DenseNet121	MNIST	3563	895	837	4506	6192	335	2027	233	3740	5377
DenseNet121	Fashion	16718	1014	551	1282	152	1945	5402	26	2114	1001
QResNet50	CIFAR10	866	1534	4375	2409	397	3127	1295	488	389	966
QGoogLeNet	CIFAR10	3612	165	1707	2336	266	348	394	600	931	1229
QDenseNet121	CIFAR10	1546	3295	1051	2794	1840	74	1021	578	705	1040
ResNet50	CIFAR10	1369	1023	1940	1278	331	2225	496	357	647	630
ResNet50	MNIST	36	7010	47	39	31	102	23	130	305	1891

## 7.3 ③ Versatile End-Goals

As mentioned earlier, the consequences BFA can cause are not limited to downgrading a classification model’s inference accuracy. We observe that BFA also shows a high potential to *manipulate* the DNN executable’s prediction results or generative outputs, and this phenomenon also extensively exists in our study.

First, in terms of classification models, Table 4 shows a summary of different predicted classes that can be controlled by single-bit BFA. When a model is pinned to a class by BFA, it has the highest probability of outputting that class for any input, granting attackers the ability to control model outputs. We notice that, for most of the models in the list, there are frequently hundreds or even thousands of vulnerable bits that can pin the model to each of the classes, although in rare cases, there will be few or no bits available for a specific class. While we do not claim this as a targeted BFA (T-BFA) in the standard sense [11] because of its non-deterministic nature, we should point out that no existing work has demonstrated practical T-BFA that can pin a model’s output using one bit, whereas all of our findings are achieved via single-bit BFA. Thus, we see this more as a “high risk, high return” strategy for sophisticated attackers.



(a) Before BFA (b) 3 Different types of outcomes after BFA

Figure 5: Output samples of DCGAN before and after BFA.

For GAN, Fig. 5(a) shows the original output of our DCGAN model before being corrupted by BFA, and Fig. 5(b) shows three different types of outcomes the model produces when given the same input after flipping three different bits in the model. Among the three types, the first one may be the most interesting: not only does it almost completely change the semantics of the output, but it also pins the model output to only two semantic classes (1 and 9). Furthermore, notice that the 9’s in the output sample have two distinct looks, suggesting that this flip is not merely causing duplications in the image pixel level, but is also manipulating the model’s learned semantics. Then, the second type degrades the output image quality while still preserving the semantics, and the third destroys both the semantics and image quality. For the first case, it is anticipated when augmenting a DNN model with this GAN under our attack, the augmented DNN will lean to predict “1” or “9” for any inputs since its training data are dominated by digit one and nine. In addition, under the last two cases, the augmented DNN should be largely downgraded because its training data are less recognizable.

## 7.4 ④ Superbits

As briefly mentioned before, during our study, we find that some vulnerable bits exist in more than one DNN executable, even though the models are trained on different datasets but just sharing the same DNN structure; we call these bits *superbits*. In Table 5, we summarize the existence of superbits over 7 different models, each trained on 3 different datasets: for each model structure, we train three versions of the model, each using a different dataset (CIFAR10, MNIST, or Fashion-MNIST); after compiling them into DNN executables, we search for superbits across all 3 executables which share the same DNN structure. For TVM-compiled executables, all of them are compiled with full optimizations and AVX2 code generation enabled. Generally, comparing with the results in Table 2, we find that about half of the vulnerable bits found in one DNN executable trained on one dataset also exist in the DNN executables trained on the other two datasets.

Since a superbit is located at the same offset and has the same flip direction in all executables that share it, an attacker will find it much more convenient to launch BFAs if she can find superbits shared by the victim DNN executable. In fact, we show in Sec. 5.1 that it is indeed feasible to find superbits that are highly likely to be shared by a set of DNN executables the attacker possesses *plus* the victim DNN executable, and

Table 5: Statistics of superbits in different DNN executables.

Model	Datasets	Compiler	#Superbits	%Superbits
ResNet50	CIFAR10 / MNIST / Fashion	TVM	4334	1.61
GoogLeNet	CIFAR10 / MNIST / Fashion	TVM	12422	1.38
DenseNet121	CIFAR10 / MNIST / Fashion	TVM	18349	1.39
ResNet50	CIFAR10 / MNIST / Fashion	TVM	7579	1.04
GoogLeNet	CIFAR10 / MNIST / Fashion	TVM	1994	0.14
DenseNet121	CIFAR10 / MNIST / Fashion	TVM	6517	0.24
ResNet50	CIFAR10 / MNIST / Fashion	Glow	5223	1.26

we describe a systematic search method to achieve this effectively and efficiently. Moreover, in Sec. 7.5, we further use the existence of superbits and our novel search method to launch practical BFAs without relying on knowledge about the victim model’s weights. Finally, in our case study in Sec. 7.6, we will provide more insights into why they can effectively disrupt the behavior even of different DNN executables.

## 7.5 ⑤ Practical Attack

This section demonstrates that practical BFAs can be launched against DNN executables. We run our experiments on a server with an Intel i7-8700 CPU and a Samsung 8GB DDR4 DRAM module without any hardware modifications. Before launching our attacks, we first extend Blacksmith to launch our RH attacks on DDR4 platforms more smoothly: in our preliminary experiments, we find that the timing function in Blacksmith is rather easily affected by noise, in the sense that it is hard to distinguish the timing difference between DRAM accesses with and without row conflicts. Thus, we replace the timing function in Blacksmith with the one in TRRespass, which we find to be more resilient to noise on our platform. Our practical attack experiment covers in total 9 different DNN executables to evaluate the attack effectiveness on different model structures, datasets, and compilers. For TVM-compiled executables, we enable full optimizations and AVX2 to better represent the real-world scenario. Then, for each executable, we launch the attack five times and collect the results.

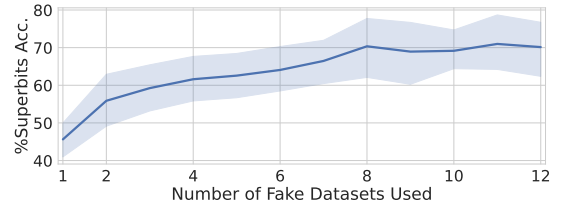


Figure 6: The relation between the number of fake datasets (Sec. 5.2) used and the accuracy of the superbits found. The line is the average for *all executables* and the shaded region shows the 95% confidence interval.

Following our attack pipeline in Sec. 5.1, we first perform memory templating by running Blacksmith with the default settings to search for the most effective access pattern on our platform and then use this pattern to sweep for flippable bit templates in a 256MB region. Totally 17,366 flippable bits are identified after about 17.5 hours, 8,855 of which are 0→1

flips. We then obtain the superbits set  $\mathcal{S}_E$  using the search method mentioned in Sec. 5; these are the bits we will attempt to flip during the attack. To empirically determine the number of “fake datasets” used to calculate  $\mathcal{S}_E$  (Sec. 5.2), we plot in Fig. 6 the relationship between the number of fake datasets used and the accuracy of the superbits found, i.e., how many bits in  $\mathcal{S}_E$  are actually also vulnerable in the victim executable. We observed that, the accuracy becomes stable at around 70% after 8 datasets, and the confidence interval is the tightest at 10 datasets. Thus, we use 10 datasets to calculate  $\mathcal{S}_E$ .

Table 6: Statistics of the 5 attack runs on 9 executables. The last row is for Glow-compiled executable whereas the rest are for TVM-compiled.

Model	Dataset	#Flips	#Crashes	%Acc. Change
ResNet50	CIFAR10	1.4	0.0	87.20 → 10.00
GoogLeNet	CIFAR10	1.4	0.0	84.80 → 10.00
DenseNet121	CIFAR10	1.0	0.0	80.00 → 11.40
DenseNet121	MNIST	1.2	0.0	99.10 → 11.20
DenseNet121	Fashion	1.2	0.0	92.50 → 10.60
QResNet50	CIFAR10	1.6	0.0	86.90 → 9.60
QGoogLeNet	CIFAR10	1.4	0.0	84.60 → 11.20
QDenseNet121	CIFAR10	1.6	0.0	78.50 → 10.20
ResNet50	CIFAR10	1.4	0.0	78.80 → 10.00

The statistics of the attack results are shown in Table 6. On average, we successfully degrade each victim executable to a random guesser (prediction accuracy of 10%) with 1.4 flip attempts while causing no crashes at all, regardless of the original prediction accuracy of the victim executable. In the case of DenseNet121 on CIFAR10, we consistently succeed with just one flip attempt in all five runs, decreasing its accuracy from 80.00% to 11.40%, ruining its inference capabilities. As for quantized models, they seem slightly more resilient to our attacks than non-quantized models, requiring 1.4 to 1.6 flips to succeed on average. In fact, in one run for the quantized DenseNet121 model, four flips were required before successfully achieving the goal. However, our results show that attacking quantized models is not a challenging target for attackers, as most quantized models are still successfully attacked within two flips. In summary, our observations suggest that BFA is a severe *and* practical threat to DNN executables.

## 7.6 Case Study

To understand the underlying root cause of how a single-bit flip is impairing the full capabilities of a DNN executable, we randomly select 60 cases, 30 each for non-superbit and superbit, from our findings. After an extensive manual study, Table 7 lists four categories of destructive consequences of single-bit corruption, including

- **Data Flow Broken:** the calculation of a specific layer’s input or output address is corrupted, resulting in reading incorrect inputs or writing layer outputs to wrong memory regions that are never read by subsequent layers.

- **Control Flow Broken:** a branch is changed to be always false, causing the corresponding calculation to be skipped and thus producing a large number of incorrect outputs.
- **Data Alignment Broken:** the offset of memory read and write instructions is deviated, causing data to be read or written in an unaligned manner.
- **Instruction Alignment Broken:** the bit flip converts alignment-purpose data bytes embedded in the .text section into instructions, causing subsequent instructions to be corrupted.

Our case study reveals common code patterns exhibited across models and datasets. Although the analyzed cases come from the same DNN executable (i.e., LeNet1), to our observation, the results are applicable to other DNN executables compiled by TVM and Glow and can offer a comprehensive understanding of the reasons behind successful BFA. Below, for each category, we discuss one representative case.

Table 7: Classification of manually analyzed BFA cases.

Bit Type	Total	Data Flow	Control Flow	Data Align	Inst Align
Non-Superbit	30	13	14	2	1
Suprbit	30	5	8	12	1

**Data Flow Broken.** We observed many different patterns of how a single bit flip could break the data flow of model inference. Here, we provide one straightforward example related to the parallelism of DNN executables. Typically, a DNN executable runs in parallel, such that multiple threads will be launched to conduct the computation of a DNN layer, while each thread will compute a portion of the output. When a thread is initialized, its corresponding output offset will be calculated according to the thread ID.

Addr	Opcode bytes	x86 assembly instruction
0xC9	4F 8D 34 64	lea r14, [r12+r12*2]
0xCD	49 C1 E6 06	shl r14, 6
0xD1	4C 03 71 10	add r14, [rcx+10h]

(a) Assembly code before BFA.

0xC9	4F AD	lodsq ;; load qword in RAX
0xCB	34 64	xor al, 64h ;; r14 not initialized
0xCD	49 C1 E6 06	shl r14, 6
0xD1	4C 03 71 10	add r14, [rcx+10h]

(b) Assembly code after BFA.

Figure 7: Case 1: the multi-thread data flow is broken.

Consider the example in Fig. 7, where  $r14$  is a register that is used to store the offset, and  $[rcx+10h]$  stores the base address of the output. Before BFA, the offset ( $r14$ ) is calculated as  $base\_address+r12*192$  ( $r12$  stores the thread ID). However, after BFA, the instruction at  $0xC9$  is split into two instructions irrelevant to  $r14$  (at  $0xC9$  and  $0xCB$ ), resulting in all threads simultaneously writing to the same output region. **Control Flow Broken.** The number of threads launched by DNN executables is determined by a predefined environment variable. When there are more threads than a DNN layer

Addr	Opcode bytes	x86 assembly instruction
0x70	83 F8 28	cmp <b>eax</b> , 28h ;; max ID
0x73	0F 4D C2	cmovge <b>eax</b> , edx ;; edx=28h
0x76	39 F0	cmp <b>eax</b> , esi ;; esi<28h
0x78	0F 8D FA 00+	jge func_end

(a) Assembly code before BFA.

0x70	83 FC 28	cmp <b>esp</b> , 28h ;; true
0x73	0F 4D C2	cmovge <b>eax</b> , edx ;; true
0x76	39 F0	cmp <b>eax</b> , esi ;; true
0x78	0F 8D FA 00+	jge func_end ;; exit
	00 00	

(b) Assembly code after BFA.

Figure 8: Case 2: the control flow is broken.

(e.g., a convolutional layer) required, redundant threads will directly jump to the function end after thread ID checking.

However, such a check is vulnerable to BFA. As shown in Fig. 8, the instruction at 0x70 originally compares 0x28 with `eax`; after BFA, it compares with `esp` register, which always stores a very large address on the stack. Thus, the following comparisons are always true, making all threads skip the execution of the function.

Opcode bytes	x86 assembly instruction
C5 FC 11+ 4C 32 C0	vmovups ymmword ptr [ <b>rdx+rsi-40h</b> ], ymm1

(a) Assembly and memory before BFA.

C5 FC 11+ 4C 32 C2	vmovups ymmword ptr [ <b>rdx+rsi-3Eh</b> ], ymm1
-----------------------	--

(b) Assembly and memory after BFA.

Figure 9: Case 3: the data alignment is broken.

**Data Alignment Broken.** In the computation of DNN executables, all floating-point numbers are represented as 4-byte aligned data. However, such alignment can be easily violated with even only a single-bit flip. As shown in Fig. 9, the `vmovups` instruction will move 32 bytes of data from the `ymm1` register to the memory. The BFA increases the offset of the target memory address by 2 bytes, resulting in unaligned data written into memory. The next time the data is read from memory in an aligned manner, the corrupted data will be interpreted as an extremely large float value (e.g.,  $1e8$ ). These large numbers will propagate in the process of DNN model inference and dominate the final result.

**Instruction Alignment Broken.** During compilation, `nop` instructions are often used to align instruction addresses. Similar cases are observed in DNN executables. Consider the example in Fig. 10, a `nop` instruction is used to align the next instruction to address 0xD0. Nevertheless, after a single-bit flip, the `nop` instruction is converted into a shorter variant, leaving its last byte (at 0xCF) being recognized as the start of an `add` instruction. The instruction alignment is thus broken, leading to an uninitialized register (`ymm0`) being used in the computation. In this case, the presence of `nan` values in `ymm0` directly destroys subsequent DNN model inference.

Addr	Opcode bytes	x86 assembly instructions
0xC8	0F 1F 84 00+	nop word ptr [ <b>rax+rax+0h</b> ]
	00 00 00 00	
0xD0	C5 FC 10 84+	vmovups ymm0, ymmword ptr
	01 30 FF FF+	[ <b>rcx+rax-0D0h</b> ]
	FF	;;load data to ymm0

(a) Assembly code before BFA.

0xC8	0F 1F 86 00+	nop dword ptr [ <b>rsi+0h</b> ]
	00 00 00	;;nop with varied length
0xCF	00 C5	add <b>ch</b> , al
0xD1	FC	cld
0xD2	10 84 01 30+	adc [ <b>rcx+rax-0D0h</b> ], al
	FF FF FF	;;leaving ymm0 uninitialized

(b) Assembly code after BFA.

Figure 10: Case 4: the instruction alignment is broken.

## 8 Discussion

**Attacking Other DNN Models.** Align with the focus of prior BFA works [28, 78], this work mostly studies CV models, including four classification models and one generative model. Production DL compilers can smoothly compile these models. In addition to that, some other types of DNN models are not discussed in this work. For instance, NLP models may take some recurrent structures, such as RNN and long short-term memory (LSTM) [27] to manage sequential inputs. We tentatively tried to evaluate our methods on them but found that TVM and Glow show immature support for RNN models. Nevertheless, our attack method should be general enough to cover RNN models since the vulnerable bits and related binary code patterns are model/operator-agnostic (see Sec. 7.6). The attack surface revealed by our attack widely exists in executables compiled from different types of DNN models.

**Countermeasures.** Our approach extensively manipulates the DNN executable outputs. Therefore, our approach may raise potential security concerns because of the wide adoption of DNN executables in business fields. Manipulating model outputs (e.g., generated images) also facilitates other attacks like training data pollution, as noted in Sec. 4. To mitigate adversarial launching BFAs, code obfuscation could be explored. Besides, since flipping vulnerable bits mainly corrupts data and control flow (as discussed in Sec. 7.6), one potential defense against BFAs might be designing DNN executable-specific data/control flow integrity [1, 10]. We leave exploring techniques to mitigate our proposed attack as future work.

## 9 Conclusion

Despite the prosperous usage of DL compilers, their security remains largely unexplored. In this paper, we have launched the first systematic study on the attack surface of BFA over DNN executables. We show that DNN executables are pervasively vulnerable to BFAs, and can be exploited in a practical, single-bit, and transferable manner. Our findings call for incorporating security mechanisms in future DL compilation toolchains.

## Acknowledgments

The authors would like to thank Patrick Jattke for providing valuable help on performing Rowhammer attack on DDR4 DRAM modules.

## References

- [1] Martín Abadi, Mihai Budiu, Ulfar Erlingsson, and Jay Ligatti. Control-flow integrity principles, implementations, and applications. *ACM Transactions on Information and System Security (TISSEC)*, 13(1):1–40, 2009.
- [2] Neha Agarwal and Thomas F Wenisch. Thermo-stat: Application-transparent page management for two-tiered main memory. In *Proceedings of the Twenty-Second International Conference on Architectural Support for Programming Languages and Operating Systems*, pages 631–644, 2017.
- [3] Amazon. Amazon SageMaker Neo uses Apache TVM for performance improvement on hardware target. <https://aws.amazon.com/sagemaker/neo/>, 2021.
- [4] Andrea Arcangeli, Izik Eidus, and Chris Wright. Increasing memory density by using ksm. In *Proceedings of the linux symposium*, pages 19–28. Citeseer, 2009.
- [5] Jiawang Bai, Baoyuan Wu, Yong Zhang, Yiming Li, Zhifeng Li, and Shu-Tao Xia. Targeted attack against deep neural networks via flipping limited weight bits. *arXiv preprint arXiv:2102.10496*, 2021.
- [6] Pierre Baldi and Peter J Sadowski. Understanding dropout. *Advances in neural information processing systems*, 26, 2013.
- [7] Lejla Batina, Shivam Bhasin, Dirmanto Jap, and Stjepan Picek. Csi nn: reverse engineering of neural network architectures through electromagnetic side channel. In *Proceedings of the 28th USENIX Conference on Security Symposium*, pages 515–532, 2019.
- [8] Tom Brown, Benjamin Mann, Nick Ryder, Melanie Subbiah, Jared D Kaplan, Prafulla Dhariwal, Arvind Neelakantan, Pranav Shyam, Girish Sastry, Amanda Askell, et al. Language models are few-shot learners. *Advances in neural information processing systems*, 33:1877–1901, 2020.
- [9] Francesco Calimeri, Aldo Marzullo, Claudio Stamile, and Giorgio Terracina. Biomedical data augmentation using generative adversarial neural networks. In *Artificial Neural Networks and Machine Learning–ICANN 2017: 26th International Conference on Artificial Neural Networks, Alghero, Italy, September 11–14, 2017, Proceedings, Part II 26*, pages 626–634. Springer, 2017.
- [10] Miguel Castro, Manuel Costa, and Tim Harris. Securing software by enforcing data-flow integrity. In *Proceedings of the 7th symposium on Operating systems design and implementation*, pages 147–160, 2006.
- [11] Huili Chen, Cheng Fu, Jishen Zhao, and Farinaz Koushanfar. Proflip: Targeted trojan attack with progressive bit flips. In *Proceedings of the IEEE/CVF International Conference on Computer Vision*, pages 7718–7727, 2021.
- [12] Tianqi Chen, Thierry Moreau, Ziheng Jiang, Lianmin Zheng, Eddie Yan, Haichen Shen, Meghan Cowan, Leyuan Wang, Yuwei Hu, Luis Ceze, et al. {TVM}: An automated end-to-end optimizing compiler for deep learning. In *13th USENIX OSDI*, pages 578–594, 2018.
- [13] Sharan Chetlur, Cliff Woolley, Philippe Vandermersch, Jonathan Cohen, John Tran, Bryan Catanzaro, and Evan Shelhamer. cuDNN: Efficient primitives for deep learning. *arXiv preprint arXiv:1410.0759*, 2014.
- [14] Lucian Cojocar, Kaveh Razavi, Cristiano Giuffrida, and Herbert Bos. Exploiting correcting codes: On the effectiveness of ecc memory against rowhammer attacks. In *2019 IEEE Symposium on Security and Privacy (SP)*, pages 55–71. IEEE, 2019.
- [15] TVM Community. Tvm deep learning compiler joins apache software foundation. <https://tvm.apache.org/2019/03/18/tvm-apache-announcement>, 2019.
- [16] Robert Elder. What causes bit flips in computer memory? <https://blog.robertelder.org/causes-of-bit-flips-in-computer-memory/#row-hammer>, 2023.
- [17] Gianni Franchi, Andrei Bursuc, Emanuel Aldea, Séverine Dubuisson, and Isabelle Bloch. Tradi: Tracking deep neural network weight distributions. In *Computer Vision–ECCV 2020: 16th European Conference, Glasgow, UK, August 23–28, 2020, Proceedings, Part XVII 16*, pages 105–121. Springer, 2020.
- [18] Maayan Frid-Adar, Idit Diamant, Eyal Klang, Michal Amitai, Jacob Goldberger, and Hayit Greenspan. Gan-based synthetic medical image augmentation for increased cnn performance in liver lesion classification. *Neurocomputing*, 321:321–331, 2018.
- [19] Pietro Frigo, Emanuele Vannacc, Hasan Hassan, Victor Van Der Veen, Onur Mutlu, Cristiano Giuffrida, Herbert Bos, and Kaveh Razavi. Trespass: Exploiting the many sides of target row refresh. In *2020 IEEE Symposium on Security and Privacy (SP)*, pages 747–762. IEEE, 2020.
- [20] Ian J Goodfellow, Jonathon Shlens, and Christian Szegedy. Explaining and harnessing adversarial examples. *arXiv preprint arXiv:1412.6572*, 2014.
- [21] Daniel Gruss, Clémentine Maurice, and Stefan Mangard. Rowhammer.js: A remote software-induced fault attack in javascript. In *Detection of Intrusions and Malware, and Vulnerability Assessment: 13th International Conference, DIMVA 2016, San Sebastián, Spain, July 7–8, 2016, Proceedings 13*, pages 300–321. Springer, 2016.

- [22] Changhee Han, Hideaki Hayashi, Leonardo Rundo, Ryosuke Araki, Wataru Shimoda, Shinichi Muramatsu, Yujiro Furukawa, Giancarlo Mauri, and Hideki Nakayama. Gan-based synthetic brain mr image generation. In *2018 IEEE 15th international symposium on biomedical imaging (ISBI 2018)*, pages 734–738. IEEE, 2018.
- [23] Red Hat. Monitoring and managing system status and performance, chapter 36. configuring huge pages. [https://access.redhat.com/documentation/en-us/red\\_hat\\_enterprise\\_linux/8/html/monitoring\\_and\\_managing\\_system\\_status\\_and\\_performance/configuring-huge-pages\\_monitoring-and-managing-system-status-and-performance](https://access.redhat.com/documentation/en-us/red_hat_enterprise_linux/8/html/monitoring_and_managing_system_status_and_performance/configuring-huge-pages_monitoring-and-managing-system-status-and-performance), 2021.
- [24] Kaiming He, Xiangyu Zhang, Shaoqing Ren, and Jian Sun. Deep residual learning for image recognition. In *CVPR*, pages 770–778, 2016.
- [25] Nishad Herath and Anders Fogh. These are not your grand daddys cpu performance counters—cpu hardware performance counters for security. *Black Hat Briefings*, 2015.
- [26] Martin Heusel, Hubert Ramsauer, Thomas Unterthiner, Bernhard Nessler, and Sepp Hochreiter. Gans trained by a two time-scale update rule converge to a local nash equilibrium. *Advances in neural information processing systems*, 30, 2017.
- [27] Sepp Hochreiter and Jürgen Schmidhuber. Long short-term memory. *Neural computation*, 1997.
- [28] Sanghyun Hong, Pietro Frigo, Yigitcan Kaya, Cristiano Giuffrida, and Tudor Dumitras. Terminal brain damage: Exposing the graceless degradation in deep neural networks under hardware fault attacks. In *USENIX Security Symposium*, pages 497–514, 2019.
- [29] Xing Hu, Ling Liang, Shuangchen Li, Lei Deng, Pengfei Zuo, Yu Ji, Xinfeng Xie, Yufei Ding, Chang Liu, Timothy Sherwood, et al. Deepsniffer: A dnn model extraction framework based on learning architectural hints. In *ASPLOS*, pages 385–399, 2020.
- [30] Texas Instruments. The AM335x microprocessors support TVM. <https://software-dl.ti.com/processor-sdk-linux/esd/docs/latest/linux/FoundationalComponents/MachineLearning/tvm.html>, 2021.
- [31] Intel. MKL-DNN for scalable deep learning. <https://software.intel.com/en-us/articles/introducing-dnn-primitives-in-intelr-mkl>, 2017.
- [32] Animesh Jain, Shoubhik Bhattacharya, Masahiro Masuda, Vin Sharma, and Yida Wang. Efficient execution of quantized deep learning models: A compiler approach. *arXiv preprint arXiv:2006.10226*, 2020.
- [33] Patrick Jattke, Victor Van Der Veen, Pietro Frigo, Stijn Gunter, and Kaveh Razavi. Blacksmith: Scalable rowhammering in the frequency domain. In *2022 IEEE Symposium on Security and Privacy (SP)*, pages 716–734. IEEE, 2022.
- [34] Dae-Hyun Kim, Prashant J Nair, and Moinuddin K Qureshi. Architectural support for mitigating row hammering in dram memories. *IEEE Computer Architecture Letters*, 14(1):9–12, 2014.
- [35] Yoongu Kim, Ross Daly, Jeremie Kim, Chris Fallin, Ji Hye Lee, Donghyuk Lee, Chris Wilkerson, Konrad Lai, and Onur Mutlu. Flipping bits in memory without accessing them: An experimental study of dram disturbance errors. *ACM SIGARCH Computer Architecture News*, 42(3):361–372, 2014.
- [36] Andrew Kwong, Daniel Genkin, Daniel Gruss, and Yuval Yarom. Rambled: Reading bits in memory without accessing them. In *2020 IEEE Symposium on Security and Privacy (SP)*, pages 695–711. IEEE, 2020.
- [37] Chris Lattner and Vikram Adve. LLVM: A compilation framework for lifelong program analysis & transformation. In *Proceedings of the International Symposium on Code Generation and Optimization: Feedback-directed and Runtime Optimization*, CGO '04, pages 75–, Washington, DC, USA, 2004. IEEE Computer Society.
- [38] Yann LeCun, Léon Bottou, Yoshua Bengio, and Patrick Haffner. Gradient-based learning applied to document recognition. *Proceedings of the IEEE*, 86(11):2278–2324, 1998.
- [39] Jinsol Lee and Ghassan AlRegib. Gradients as a measure of uncertainty in neural networks. In *2020 IEEE International Conference on Image Processing (ICIP)*, pages 2416–2420. IEEE, 2020.
- [40] Moritz Lipp, Michael Schwarz, Lukas Raab, Lukas Lamster, Misiker Tadesse Aga, Clémentine Maurice, and Daniel Gruss. Nethammer: Inducing rowhammer faults through network requests. In *2020 IEEE European Symposium on Security and Privacy Workshops (EuroS&PW)*, pages 710–719. IEEE, 2020.
- [41] Yizhi Liu, Yao Wang, Ruofei Yu, Mu Li, Vin Sharma, and Yida Wang. Optimizing {CNN} model inference on cpus. In *USENIX ATC*, pages 1025–1040, 2019.
- [42] Lingxiao Ma, Zhiqiang Xie, Zhi Yang, Jilong Xue, Youshan Miao, Wei Cui, Wenxiang Hu, Fan Yang, Lintao Zhang, and Lidong Zhou. Rammer: Enabling holistic deep learning compiler optimizations with rtasks. In *14th USENIX OSDI*, pages 881–897, 2020.
- [43] Ali Madani, Mehdi Moradi, Alexandros Karargyris, and Tanveer Syeda-Mahmood. Chest x-ray generation and data augmentation for cardiovascular abnormality classification. In *Medical imaging 2018: Image processing*, volume 10574, pages 415–420. SPIE, 2018.

- [44] Hartmut Maennel, Ibrahim M Alabdulmohsin, Ilya O Tolstikhin, Robert Baldock, Olivier Bousquet, Sylvain Gelly, and Daniel Keysers. What do neural networks learn when trained with random labels? *Advances in Neural Information Processing Systems*, 33:19693–19704, 2020.
- [45] Timothy Prickett Morgan. INSIDE FACEBOOK’S FUTURE RACK AND MICROSERVER IRON. <https://www.nextplatform.com/2020/05/14/inside-facebooks-future-rack-and-microserver-iron/>, 2020.
- [46] Nvidia. NVVM IR. <https://docs.nvidia.com/cuda/nvvm-ir-spec/index.html>, 2021.
- [47] NXP. NXP uses Glow to optimize models for low-power NXP MCUs. <https://www.nxp.com/company/blog/glow-compiler-optimizes-neural-networks-for-low-power-nxp-mcus:BL-OPTIMIZES-NEURAL-NETWORKS>, 2020.
- [48] OctoML. OctoML leverages TVM to optimize and deploy models. <https://octoml.ai/features/maximize-performance/>, 2021.
- [49] Nicolas Papernot, Patrick McDaniel, Ian Goodfellow, Somesh Jha, Z Berkay Celik, and Ananthram Swami. Practical black-box attacks against machine learning. In *ACM Asia CCS*, pages 506–519, 2017.
- [50] Georg Pichler, Pierre Jean A Colombo, Malik Boudiaf, Günther Koliander, and Pablo Piantanida. A differential entropy estimator for training neural networks. In *International Conference on Machine Learning*, pages 17691–17715. PMLR, 2022.
- [51] Vinaychandran Pondenkandath, Michele Alberti, Sammer Puran, Rolf Ingold, and Marcus Liwicki. Leveraging random label memorization for unsupervised pre-training. *Workshop of Integration of Deep Learning Theories at Conference on Neural Information Processing Systems (NIPS)*, 2018.
- [52] Ivan Puddu, Moritz Schneider, Daniele Lain, Stefano Boschetto, and Srdjan Čapkun. On (the lack of) code confidentiality in trusted execution environments. *arXiv preprint arXiv:2212.07899*, 2022.
- [53] Pytorch. Dense Convolutional Network (DenseNet). [https://pytorch.org/hub/pytorch\\_vision\\_densenet/](https://pytorch.org/hub/pytorch_vision_densenet/), 2021.
- [54] Qualcomm. Qualcomm contributes Hexagon DSP improvements to the Apache TVM community. <https://developer.qualcomm.com/blog/tvm-open-source-compiler-now-includes-initial-support-qualcomm-hexagon-dsp>, 2020.
- [55] Alec Radford, Luke Metz, and Soumith Chintala. Unsupervised representation learning with deep convolutional generative adversarial networks. *arXiv preprint arXiv:1511.06434*, 2015.
- [56] Adnan Siraj Rakin, Md Hafizul Islam Chowdhury, Fan Yao, and Deliang Fan. Deepsteal: Advanced model extractions leveraging efficient weight stealing in memories. In *2022 IEEE Symposium on Security and Privacy (SP)*, pages 1157–1174. IEEE, 2022.
- [57] Adnan Siraj Rakin, Zhezhi He, and Deliang Fan. Bit-Flip Attack: Crushing Neural Network With Progressive Bit Search. In *2019 IEEE/CVF International Conference on Computer Vision (ICCV)*, pages 1211–1220. IEEE.
- [58] Adnan Siraj Rakin, Zhezhi He, and Deliang Fan. Bit-flip attack: Crushing neural network with progressive bit search. In *Proceedings of the IEEE/CVF International Conference on Computer Vision*, pages 1211–1220, 2019.
- [59] Adnan Siraj Rakin, Zhezhi He, and Deliang Fan. Tbt: Targeted neural network attack with bit trojan. In *Proceedings of the IEEE/CVF Conference on Computer Vision and Pattern Recognition*, pages 13198–13207, 2020.
- [60] Adnan Siraj Rakin, Zhezhi He, Jingtao Li, Fan Yao, Chaitali Chakrabarti, and Deliang Fan. T-bfa: Targeted bit-flip adversarial weight attack. *IEEE Transactions on Pattern Analysis and Machine Intelligence*, 44(11):7928–7939, 2021.
- [61] Adnan Siraj Rakin, Yukui Luo, Xiaolin Xu, and Deliang Fan. Deep-dup: An adversarial weight duplication attack framework to crush deep neural network in multi-tenant fpga. In *30th USENIX Security Symposium*, 2021.
- [62] Kaveh Razavi, Ben Gras, Cristiano Giuffrida, Erik Bosman, Bart Preneel, and Herbert Bos. Flip Feng Shui: Hammering a Needle in the Software Stack. page 19.
- [63] Nadav Rotem, Jordan Fix, Saleem Abdulrasool, Garret Catron, Summer Deng, Roman Dzhabarov, Nick Gibson, James Hegeman, Meghan Lele, Roman Levenstein, et al. Glow: Graph lowering compiler techniques for neural networks. *arXiv preprint*, 2018.
- [64] Divyanshu Saxena, Tao Ji, Arjun Singhvi, Junaid Khalid, and Aditya Akella. Memory deduplication for serverless computing with medes. In *Proceedings of the Seventeenth European Conference on Computer Systems*, pages 714–729, 2022.
- [65] Mark Seaborn and Thomas Dullien. Exploiting the dram rowhammer bug to gain kernel privileges. *Black Hat*, 15:71, 2015.
- [66] Connor Shorten and Taghi M Khoshgoftaar. A survey on image data augmentation for deep learning. *Journal of big data*, 6(1):1–48, 2019.
- [67] Karen Simonyan and Andrew Zisserman. Very deep convolutional networks for large-scale image recognition. *arXiv preprint arXiv:1409.1556*, 2014.

- [68] Youssef Skandarani, Pierre-Marc Jodoin, and Alain Lalande. Gans for medical image synthesis: An empirical study. *Journal of Imaging*, 9(3):69, 2023.
- [69] Ken Thompson. Reflections on trusting trust. *Communications of the ACM*, 27(8):761–763, 1984.
- [70] Florian Tramèr, Fan Zhang, Ari Juels, Michael K Reiter, and Thomas Ristenpart. Stealing machine learning models via prediction apis. In *USENIX Sec’16*.
- [71] Victor van der Veen, Yanick Fratantonio, Martina Lindorfer, Daniel Gruss, Clémentine Maurice, Giovanni Vigna, Herbert Bos, Kaveh Razavi, and Cristiano Giuffrida. Drammer: Deterministic Rowhammer Attacks on Mobile Platforms. In *Proceedings of the 2016 ACM SIGSAC Conference on Computer and Communications Security*, pages 1675–1689. ACM.
- [72] Victor Van Der Veen, Yanick Fratantonio, Martina Lindorfer, Daniel Gruss, Clémentine Maurice, Giovanni Vigna, Herbert Bos, Kaveh Razavi, and Cristiano Giuffrida. Drammer: Deterministic rowhammer attacks on mobile platforms. In *Proceedings of the 2016 ACM SIGSAC conference on computer and communications security*, pages 1675–1689, 2016.
- [73] Victor Van der Veen, Martina Lindorfer, Yanick Fratantonio, Harikrishnan Padmanabha Pillai, Giovanni Vigna, Christopher Kruegel, Herbert Bos, and Kaveh Razavi. Guardion: Practical mitigation of dma-based rowhammer attacks on arm. In *Detection of Intrusions and Malware, and Vulnerability Assessment: 15th International Conference, DIMVA 2018, Saclay, France, June 28–29, 2018, Proceedings 15*, pages 92–113. Springer, 2018.
- [74] Ashish Vaswani, Noam Shazeer, Niki Parmar, Jakob Uszkoreit, Llion Jones, Aidan N Gomez, Łukasz Kaiser, and Illia Polosukhin. Attention is all you need. In *Advances in neural information processing systems*, pages 5998–6008, 2017.
- [75] Jialai Wang, Ziyuan Zhang, Meiqi Wang, Han Qiu, Tianwei Zhang, Qi Li, Zongpeng Li, Tao Wei, and Chao Zhang. Aegis: Mitigating targeted bit-flip attacks against deep neural networks. *arXiv preprint arXiv:2302.13520*, 2023.
- [76] Sally Ward-Foxton. Google and Nvidia Tie in MLPerf; Graphcore and Habana Debut. <https://www.eetimes.com/google-and-nvidia-tie-in-mlperf-graphcore-and-habana-debut/#>, 2021.
- [77] Mengjia Yan, Christopher W Fletcher, and Josep Torrellas. Cache telepathy: Leveraging shared resource attacks to learn dnn architectures. In *USENIX Sec’20*.
- [78] Fan Yao, Adnan Siraj Rakin, and Deliang Fan. DeepHammer: Depleting the Intelligence of Deep Neural Networks through Targeted Chain of Bit Flips. pages 1463–1480.
- [79] Honggang Yu, Haocheng Ma, Kaichen Yang, Yiqiang Zhao, and Yier Jin. Deepem: Deep neural networks model recovery through em side-channel information leakage. In *2020 IEEE International Symposium on Hardware Oriented Security and Trust (HOST)*, pages 209–218. IEEE, 2020.
- [80] Richard Zhang, Phillip Isola, Alexei A Efros, Eli Shechtman, and Oliver Wang. The unreasonable effectiveness of deep features as a perceptual metric. In *Proceedings of the IEEE conference on computer vision and pattern recognition*, pages 586–595, 2018.
- [81] Ranyang Zhou, Sabbir Ahmed, Adnan Siraj Rakin, and Shaahin Angizi. Dnn-defender: An in-dram deep neural network defense mechanism for adversarial weight attack. *arXiv preprint arXiv:2305.08034*, 2023.
- [82] Yuankun Zhu, Yueqiang Cheng, Husheng Zhou, and Yantao Lu. Hermes attack: Steal {DNN} models with lossless inference accuracy. In *USENIX Security*, 2021.